

# A Stable Silylene in a Reactive Environment: Synthesis, Reactivity, and Silicon Extrusion Chemistry of a Coordinatively Unsaturated Ruthenium Silylene Complex Containing Chloride and $\eta^3\text{-P-C-P}$ Ligands

Dino Amoroso,<sup>†</sup> Michael Haaf,<sup>S,†</sup> Glenn P. A. Yap,<sup>†</sup> Robert West,<sup>S</sup> and Deryn E. Fogg<sup>\*,†</sup>

Center for Catalysis Innovation and Research, Department of Chemistry, University of Ottawa, Ottawa, Ontario, Canada K1N 6N5, and Organosilicon Research Center, Department of Chemistry, University of Wisconsin, Madison, Wisconsin 53706

Received March 7, 2001

Reaction of  $[(\text{dcypb})\text{ClRu}(\mu\text{-Cl})_3\text{Ru}(\text{dcypb})(\text{N}_2)]$  (**1**) with 4 equiv of the stable silylene 1,3-di-*tert*-butyl-1,3,2-diazasilol-2-ylidene ( $\text{SiL}^{\text{N}_2}$ ) yields coordinatively unsaturated  $\text{RuCl}(\eta^3\text{-dcypb})(\text{SiL}^{\text{N}_2})$  (**2**). Complex **2** is a rare example of a trans-spanning diphosphine complex, this geometry resulting from an unprecedented attack of the metal on the tetramethylene ligand backbone. X-ray and solid-state  $^{31}\text{P}$  NMR and IR analysis reveal an agostic interaction between the metal and a silylene  $\text{Bu}^t$  group. In solution, this interaction is observed only at low temperature. Reaction of **2** with  $\text{H}_2$  containing trace  $\text{H}_2\text{O}$  yields siloxane dimer  $[\text{L}^{\text{N}_2}\text{Si}(\text{H})_2\text{O}]_2$  (**3**) and the ruthenium hydride- $\text{H}_2$  adduct  $[(\text{dcypb})(\text{H})\text{Ru}(\mu\text{-Cl})_2(\mu\text{-H})\text{Ru}(\text{dcypb})(\text{H}_2)]$  (**4**). Attempts to isolate **4** resulted in serendipitous crystallization of decomposition product **5**,  $[(\text{dcypb})(\text{H})\text{Ru}(\mu\text{-Cl})_3\text{Ru}(\text{dcypb})(\text{N}_2)]$ . X-ray analysis of **5** revealed a structure closely analogous to that of **4**, in which bridging hydride is replaced by chloride, and  $\eta^2\text{-H}_2$  by  $\eta^2\text{-N}_2$ . Displacement of silylene from **2** is facile: treatment with 1 atm of CO affords free  $\text{SiL}^{\text{N}_2}$ , accompanied by  $\text{RuCl}(\eta^3\text{-dcypb})(\text{CO})_2$  as a mixture of three isomers (**6–8**).

## Introduction

Transition-metal derivatives of silylenes are of intense interest for their potential relevance to a range of organosilicon transformations, and development of routes to such complexes has provided a rich area of inquiry. Synthetic strategies focus on reactions of coordinatively unsaturated precursors with a stable silylene<sup>1–6</sup> or generation and installation of the silylene in situ,<sup>7–10</sup>

including by 1,2-migration from silyl hydrides.<sup>11</sup> Particularly well developed is the coordination chemistry<sup>1–4,6</sup> of 1,3-di-*tert*-butyl-1,3,2-diazasilol-2-ylidene ( $\text{SiL}^{\text{N}_2}$ ), the first isolated example of a stable silylene, reported by Denk and West in 1994.<sup>12</sup> This compound can be recognized as a silicon analogue of the stable N-heterocyclic carbene ligands (“Arduengo carbenes”),<sup>13</sup> which have recently attained a high profile in Ru-catalyzed metathesis reactions. Irrespective of installation route, the stability of the *bound* silylene is typically ensured by use of “innocent” ligands, noncoordinating anions, and a coordinatively saturated metal. With few exceptions,<sup>3,5,14</sup> common catalytically relevant ligands such as chloride, hydride, or phosphine have been neglected. In the course of studies directed at the design of novel ruthenium metathesis catalysts,<sup>15,16</sup> we developed facile routes to chlororuthenium complexes containing the electron-rich chelating phosphine

\* Corresponding author. E-mail: dfogg@science.uottawa.ca. Fax: (613) 562-5170.

<sup>†</sup> University of Ottawa.

<sup>S</sup> University of Wisconsin.

<sup>‡</sup> Present address: Department of Chemistry and Biochemistry, Elizabethtown College, One Alpha Drive, Elizabethtown, PA 17022.

(1) (a) Haaf, M.; Schmedake, T. A.; West, R. *Acc. Chem. Res.* **2000**, *33*, 704. (b) Schmedake, T. A.; Haaf, M.; Paradise, B. J.; Millevolte, A. J.; Powell, D. R.; West, R. *J. Organomet. Chem.* **2001**, *636*, 17.

(2) Schmedake, T. A.; Haaf, M.; Paradise, B. J.; Powell, D.; West, R. *Organometallics* **2000**, *19*, 3263.

(3) Dysard, J. M.; Tilley, T. D. *Organometallics* **2000**, *19*, 4726.

(4) Denk, M.; Hayashi, R. K.; West, R. *J. Chem. Soc., Chem. Commun.* **1994**, 33.

(5) Gehrhuss, B.; Hitchcock, P. B.; Lappert, M. F.; Maciejewski, H. *Organometallics* **1998**, *17*, 5599.

(6) Petri, S. H. A.; Eikenberg, D.; Neumann, B.; Stammer, H. G.; Jutz, P. *Organometallics* **1999**, *18*, 2615.

(7) (a) Tilley, T. D. *The Chemistry of Organic-Silicon Compounds*; Patai, S., Rappoport, Z., Eds.; Wiley: New York, 1989; Vol. 2, Chapter 24, p 1415. (b) Tilley, T. D. *The Silicon-Heteroatom Bond*; Patai, S., Rappoport, Z., Eds.; Wiley: New York, 1991; Chapters 9 and 10, pp 245 and 309.

(8) (a) Wanandi, P. W.; Glaser, P. B.; Tilley, T. D. *J. Am. Chem. Soc.* **2000**, *122*, 972. (b) Grubine, S. K.; Tilley, T. D.; Arnold, F. P.; Rheingold, A. L. *J. Am. Chem. Soc.* **1994**, *116*, 5495. (c) Grubine, S. D.; Tilley, T. D. *J. Am. Chem. Soc.* **1993**, *115*, 7884. (d) Straus, D. A.; Tilley, T. D. *J. Am. Chem. Soc.* **1987**, *109*, 5872.

(9) Straus, D. A.; Grubine, S. D.; Tilley, T. D. *J. Am. Chem. Soc.* **1990**, *112*, 7801.

(10) Grubine, S. K.; Mitchell, G. P.; Straus, D. A.; Tilley, T. D.; Rheingold, A. L. *Organometallics* **1998**, *17*, 5607.

(11) Mitchell, G. P.; Tilley, T. D. *Angew. Chem., Int. Ed. Engl.* **1998**, *37*, 2524.

(12) Denk, M.; Lennon, R.; Hayashi, R.; West, R.; Belyakov, A. V.; Verne, H. P.; Haaland, A.; Wagner, M.; Metzler, N. *J. Am. Chem. Soc.* **1994**, *116*, 2691.

(13) Arduengo, A. J.; Dias, H. V. R.; Harlow, R. L.; Kline, M. *J. Am. Chem. Soc.* **1992**, *114*, 5530.

(14) Jutz, P.; Mohrke, A. *Angew. Chem., Int. Ed. Engl.* **1990**, *29*, 893.

(15) Amoroso, D.; Fogg, D. E. *Can. J. Chem.* **2001**, *79*, 958.

(16) Amoroso, D.; Fogg, D. E. *Macromolecules* **2000**, *33*, 2815.

dcbp (dcbp = bis(dicyclohexyl)-1,4-phosphinobutane,  $\text{Cy}_2\text{P}(\text{CH}_2)_4\text{PCy}_2$ ), which displays a rich coordination chemistry.<sup>15</sup> We were thus interested in examining the properties of the  $\text{SiL}^{\text{N}_2}$  ligand within this coordinatively unsaturated metal environment.

## Experimental Section

**General Procedures.** All reactions were carried out under  $\text{N}_2$  using standard Schlenk or drybox techniques, unless otherwise noted. Hydrogen (Praxair UHP Grade) and deuterium (Aldrich 99.8%) were purified by passage through a Deoxo cartridge and an indicating Drierite column in series. CO (Praxair) was passed through Drierite only. Dry, oxygen-free solvents were obtained using an Anhydrous Engineering solvent purification system and stored over Linde 4 Å molecular sieves.  $\text{C}_6\text{D}_6$  and toluene- $d_8$  were dried over activated sieves (Linde 4 Å) and degassed by consecutive freeze/pump/thaw cycles.  $\text{Ru}_2\text{Cl}_4(\text{dcbp})_2(\text{N}_2)$  (**1**) was prepared as previously described.<sup>15</sup>  $^1\text{H}$  NMR (200 or 500 MHz) spectra were recorded on a Varian Gemini 200 or Bruker AMX-500 spectrometer. Solution  $^{31}\text{P}$  NMR (121 MHz),  $^{13}\text{C}$  NMR (75 MHz), and  $^{29}\text{Si}$  NMR (58 MHz) spectra were recorded on a Varian XL-300 MHz spectrometer; solid-state NMR spectra, on a Bruker ASX-200 MHz spectrometer (81 MHz for  $^{31}\text{P}$ ). All 2D experiments were carried out on the AMX-500 instrument. IR spectra were measured on a Bomem MB100 IR spectrometer. Microanalytical data were obtained using a Perkin-Elmer Series II CHNS/O instrument. Computational results were obtained using the Cerius<sup>2</sup>-DMol<sup>3</sup> molecular modeling suite from Molecular Simulations Inc.<sup>17</sup> Density functional theory (DFT) calculations were carried out with a Double Numerical basis set and Perdew–Wang local correlation using the default grid.

**$\text{RuCl}(\eta^3\text{-dcbp})(\text{SiL}^{\text{N}_2})$  (**2**).** Reaction of **1** (0.198 g, 0.314 mmol Ru) with  $\text{SiL}^{\text{N}_2}$  (0.127 g, 0.647 mmol) in  $\text{C}_6\text{H}_6$  (10 mL) at 50 °C gave a homogeneous deep red/brown solution over 4 h. Concentration and addition of cold hexanes afforded a yellow precipitate, which was reprecipitated from benzene–hexanes. Yield after drying under vacuum: 0.199 g (81%).  $^1\text{H}$  NMR ( $\delta$ ,  $\text{C}_6\text{D}_6$ ): 6.33 (d, olefinic, 1H,  $^2J_{\text{HH}} = 3.8$  Hz), 6.17 (d, olefinic, 1H,  $^2J_{\text{HH}} = 3.8$  Hz), 3.2–3.4 (m, aliphatic, 2H), 2.8–3.0 (m, aliphatic, 2H), 1.0–2.7 (br m, aliphatic, 47H), 1.29 (s,  $\text{Bu}^t$ , 9H), 1.01 (s,  $\text{Bu}^t$ , 9H).  $^{31}\text{P}\{^1\text{H}\}$  NMR ( $\delta$ ,  $\text{C}_6\text{D}_6$ ): 60.2 (d,  $\text{CH}_2\text{CH}_2\text{P}$ ,  $^2J_{\text{PP}} = 263$  Hz), –10.3 (d,  $\text{CHCH}_2\text{P}$ ,  $^2J_{\text{PP}} = 263$  Hz). Solid-state  $^{31}\text{P}$  NMR (80.9 MHz): 56.2 (d,  $\text{CH}_2\text{CH}_2\text{P}$ ,  $^2J_{\text{PP}} = 267$  Hz), –11.6 (d,  $\text{CHCH}_2\text{P}$ ,  $^2J_{\text{PP}} = 267$  Hz).  $^{29}\text{Si}\{^1\text{H}\}$  NMR ( $\delta$ ,  $\text{C}_6\text{D}_6$ ): 105.7 ppm (t,  $^2J_{\text{PSi}} = 32$  Hz). IR (Nujol):  $\nu(\text{C-H})$  2923, 2853, 2727, 2668  $\text{cm}^{-1}$ ; (benzene): 2924, 2851  $\text{cm}^{-1}$ . The extreme air-sensitivity of the complex resulted in fuming and immediate decomposition to a dark brown powder on attempted combustion analysis, giving data consistently low in carbon. Crystals of **2** were obtained by slow evaporation of a benzene solution.

**Reaction of **2** with  $\text{H}_2$ .** A solution of **2** (62 mg, 0.08 mmol) in 5 mL of  $\text{C}_6\text{H}_6$  was warmed at 50 °C for 24 h under  $\text{H}_2$ . Conversion of  $\text{SiL}^{\text{N}_2}$  to siloxane dimer  $[\text{L}^{\text{N}_2}\text{Si}(\text{H})_2\text{O}]_2$  **3** was confirmed by detailed spectroscopic analysis (see text), reinforced by comparison with literature values.<sup>18</sup> The inorganic product is spectroscopically identical to Ru species  $\text{Ru}(\text{dcbp})(\text{H})(\mu\text{-Cl})_2(\mu\text{-H})\text{Ru}(\text{dcbp})(\text{H}_2)$  **4**, prepared by reaction of **1** with potassium tri(*sec*-butyl)borohydride.<sup>19</sup> Its isolation was thwarted by decomposition problems, including dehydrogenation, as indicated by the appearance of olefinic signals and a peak for dissolved  $\text{H}_2$  by  $^1\text{H}$  NMR (see text). Solution  $^{31}\text{P}\{^1\text{H}\}$  NMR ( $\delta$ ,

$\text{C}_6\text{D}_6$ ): 65.1 (br s), 52.2 (br s), ratio 1:1.  $^1\text{H}$  NMR ( $\delta$ ,  $\text{C}_6\text{D}_6$ ): 5.95 (s, SiH), 5.80 (s, olefinic), 0.6–3.0 (m, aliphatic, **3**, **4**), –13.8 (br s,  $\text{RuH}$ ,  $\text{Ru}(\text{H}_2)$ , **4**).

**Reaction of **2** with  $\text{D}_2$ .** Deuterium gas was bubbled through a solution of **2** (10 mg, 12.8  $\mu\text{mol}$ ) in  $\text{C}_6\text{H}_6$  (1 mL) in a Teflon-lined screw-cap NMR tube (2 min). The sealed tube was warmed at 50 °C for 24 h under  $\text{D}_2$ .  $^2\text{H}$  NMR ( $\delta$ ,  $\text{C}_6\text{H}_6$ ): 5.95 (s, SiD), 0.5–3.0 (br m, aliphatic, **4-d**), –13.8 (br s,  $\text{RuD}$ ,  $\text{Ru}(\text{D}_2)$ , **4-d**).  $^{31}\text{P}$  NMR ( $\delta$ ,  $\text{C}_6\text{H}_6$ ): 65.1 (br s), 52.2 (br s); ratio 1:1.

**Room-Temperature Reaction of **2** with  $\text{D}_2$ .** Deuterium gas was bubbled through a solution of **2** (10 mg, 12.8  $\mu\text{mol}$ ) in  $\text{C}_6\text{H}_6$  (1 mL) in a Teflon-lined screw-cap NMR tube (2 min). The sealed tube was stored at RT under  $\text{D}_2$ , and the reaction monitored by  $^2\text{H}$  and  $^{31}\text{P}$  NMR. After 48 h signals for **4-d** were visible, accompanying those for **2**. No incorporation of deuterium into the diphosphine backbone was observed prior to formation of **4-d**.

**Reaction of **2** with  $\text{H}_2\text{O}$ .** To a solution of **2** (10 mg, 12.8  $\mu\text{mol}$ ) in  $\text{C}_6\text{D}_6$  (1 mL) under  $\text{N}_2$  in a Teflon-lined screw-cap NMR tube was added degassed  $\text{H}_2\text{O}$  (0.23  $\mu\text{L}$ , 12.8  $\mu\text{mol}$ ). After 2 h at RT, <20% of **2** remained ( $^1\text{H}$ ,  $^{31}\text{P}$  NMR); several new products were evident, of which only 15% of the integrated intensity could be ascribed to **4**. The tube was then purged with  $\text{H}_2$ . After 4 h, no **2** remained and the major product (50% of integrated intensity) was **4**. No further changes were observed over 24 h.

**Reaction of **2** with  $\text{H}_2\text{O}$  and  $\text{H}_2$ .** To a solution of **2** (10 mg, 12.8  $\mu\text{mol}$ ) in  $\text{C}_6\text{D}_6$  (1 mL) in a Teflon-lined screw-cap NMR tube was added degassed  $\text{H}_2\text{O}$  (0.23  $\mu\text{L}$ , 12.8  $\mu\text{mol}$ ). The sealed tube was immediately purged with  $\text{H}_2$ . Conversion to **4** and siloxane **3** was complete within 6 h at RT ( $^1\text{H}$ ,  $^{31}\text{P}$  NMR).

**$[(\text{dcbp})(\text{H})\text{Ru}(\mu\text{-Cl})_2\text{Ru}(\text{dcbp})(\text{N}_2)]$  (**5**).** Complex **5** was serendipitously obtained on attempted isolation of **4** from the reaction of **2** with  $\text{H}_2$ . A benzene solution containing the reaction products was reduced to an orange residue under vacuum, washed with hexanes, and redissolved in benzene.  $^{31}\text{P}$  NMR analysis revealed the presence of many products, including **4**, characterized by resonances (many of which were broad) between 87 and 2 ppm.  $^1\text{H}$  NMR, hydride region:  $\delta$  –19.5 to –20.6 (overlapping multiplets), –13.8 (br s, **4**), –11 to –12 (two broad singlets). Small crystals of **5** deposited on slow evaporation.

**Reaction of **2** with CO.** A suspension of **2** (86 mg, 0.11 mmol) in 0.75 mL of toluene- $d_8$  gave a homogeneous pale yellow solution on stirring under 1 atm of CO.  $^1\text{H}$  NMR showed complete loss of signals for bound silylene within 24 h and a large singlet for free  $\text{SiL}^{\text{N}_2}$ . Three products evident by  $^{31}\text{P}$  NMR were identified as isomeric  $\text{Ru}(\eta^3\text{-dcbp})(\text{CO})_2$  species **6–8** (see text). The high solubility of **6–8** in all solvents, including hexanes, precluded separation from free silylene.  $^1\text{H}$  NMR ( $\delta$ ,  $\text{C}_6\text{D}_6$ ): 6.75 (s, olefinic, 2H), 0.8–3.4 (br, m, 51H), 1.40 (s,  $\text{Bu}^t$ , 18H).  $^{31}\text{P}\{^1\text{H}\}$  NMR ( $\delta$ ,  $\text{C}_6\text{D}_6$ ): 77.6 (d,  $\text{CH}_2\text{CH}_2\text{P}$ ,  $^2J_{\text{PP}} = 249$  Hz, **6** or **7**), 74.4 (d,  $\text{CH}_2\text{CH}_2\text{P}$ ,  $^2J_{\text{PP}} = 246$  Hz, **6** or **7**), 72.9 (d,  $\text{CH}_2\text{CH}_2\text{P}$ ,  $^2J_{\text{PP}} = 164$  Hz, **8**), –29.0 (d,  $\text{CHCH}_2\text{P}$ ,  $^2J_{\text{PP}} = 249$  Hz, **6** or **7**), –29.9 (d,  $\text{CHCH}_2\text{P}$ ,  $^2J_{\text{PP}} = 246$  Hz, **6** or **7**), –38.2 (d,  $\text{CHCH}_2\text{P}$ ,  $^2J_{\text{PP}} = 164$  Hz, **8**). IR (Nujol,  $\nu(\text{CO})$ ,  $\text{cm}^{-1}$ ): 2010, 1925, 1880.

**Reaction of **2** with  $^{13}\text{C}$ CO.** The reaction was carried out as above to afford the corresponding  $^{13}\text{C}$  isotopomers, **6'–8'**. Peak doubling in the  $^{31}\text{P}$  NMR spectrum due to  $^{13}\text{C}$ – $^{31}\text{P}$  coupling confirms the presence of two carbonyl ligands in each molecule, though second-order effects limit rigorous analysis of the  $^{13}\text{C}$  NMR spectrum.  $^{31}\text{P}\{^1\text{H}\}$  NMR ( $\delta$ ,  $\text{C}_6\text{D}_6$ ): 77.6 (ddd,  $\text{CH}_2\text{CH}_2\text{P}$ ,  $^2J_{\text{PP}} = 249$  Hz,  $^2J_{\text{PC}} = 12$  Hz,  $^2J_{\text{PC}} = 4.2$  Hz, **6'** or **7'**), 74.4 (ddd,  $\text{CH}_2\text{CH}_2\text{P}$ ,  $^2J_{\text{PP}} = 246$  Hz,  $^2J_{\text{PC}} = 11.6$  Hz,  $^2J_{\text{PC}} = 4.6$  Hz, **6'** or **7'**), 72.9 (dt,  $\text{CH}_2\text{CH}_2\text{P}$ , **8'**,  $^2J_{\text{PP}} = 164$  Hz,  $^2J_{\text{PC}} = 13.2$  Hz), –29.0 (ddd,  $\text{CH}_2\text{CH}_2\text{P}$ ,  $^2J_{\text{PP}} = 249$  Hz,  $^2J_{\text{PC}} = 13.4$  Hz,  $^2J_{\text{PC}} = 4.9$  Hz, **6'** or **7'**), –29.9 (ddd,  $\text{CH}_2\text{CH}_2\text{P}$ ,  $^2J_{\text{PP}} = 246$  Hz,  $^2J_{\text{PC}} = 11.5$  Hz,  $^2J_{\text{PC}} = 3.6$  Hz, **6'** or **7'**), –38.2 (dt,  $\text{CH}_2\text{CH}_2\text{P}$ , **8'**,  $^2J_{\text{PP}} = 164$  Hz,  $^2J_{\text{PC}} = 13.4$  Hz).  $^{13}\text{C}\{^1\text{H}\}$  NMR ( $\delta$ ,  $\text{C}_6\text{D}_6$ ; CO

(17) Cerius<sup>2</sup> Property Prediction, Molecular Simulations Inc.: San Diego, 1999.

(18) Haaf, M.; Schmiedl, A.; Schmedake, T. A.; Powell, D. R.; Millevolte, A. J.; Denk, M.; West, R. *J. Am. Chem. Soc.* **1998**, *120*, 12714.

(19) Amoroso, D.; Fogg, D. E. *Organometallics*, submitted.



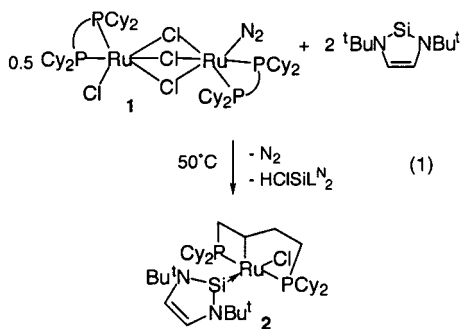
region only): 214.6 (m), 210.4 (m), 205.9 (m), 202.3 (m), 201.7 (m), 198.9 (m), 198.2 (m).

**Structural Determinations of 2 and 5.** Suitable crystals were selected, mounted on thin glass fibers using paraffin oil, and cooled to the data collection temperature. Data were collected on a Bruker AX SMART 1k CCD diffractometer using  $0.3^\circ$   $\omega$ -scans at  $0^\circ$ ,  $90^\circ$ , and  $180^\circ$  in  $\phi$ . Unit-cell parameters were determined from 60 data frames collected at different sections of the Ewald sphere. Semiempirical absorption corrections based on equivalent reflections were applied.<sup>20</sup>

Systematic absences in the diffraction data and unit-cell parameters for **2** were consistent with space groups  $Pc$  (No. 7) and  $P2_1/c$  (13). Only the solution in the acentric space group option yielded chemically reasonable and computationally stable results of refinement with a packing diagram that does not display any overlooked crystal symmetry. A nil Flack parameter indicates the true hand of the data set had been determined. In analysis of **5**, no symmetry higher than triclinic was observed, and solution in the centrosymmetric option yielded chemically reasonable and computationally stable results of refinement. Both structures were solved by direct methods, completed with difference Fourier syntheses, and refined with full-matrix least-squares procedures based on  $F^2$ . Two symmetry-unique but chemically equivalent compound molecules were located in the asymmetric unit of **2**. One cyclohexyl group in **2** displays distorted ellipsoids, suggesting conformational disorder, but attempts to model the disorder were unsatisfactory. A cocrystallized benzene molecule was located in the asymmetric unit of **5**. The hydride ligand in **5** could not be located and was ignored except in the calculation of intrinsic properties. All non-hydrogen atoms were refined with anisotropic displacement parameters. All hydrogen atoms on organic moieties were treated as idealized contributions. All scattering factors and anomalous dispersion factors are contained in the SHEXTL 5.10 program library.<sup>21</sup>

## Results and Discussion

We recently reported a high-yield route to chloride-bridged ruthenium species **1**, a synthetically valuable source of the  $\text{RuCl}_2(\text{dcypb})$  fragment.<sup>15</sup> A suspension of **1** in benzene reacts with  $\text{SiL}^{\text{N}_2}$  within 4 h at  $50^\circ\text{C}$ , yielding a homogeneous orange solution in which **2** is the sole Ru-containing product (eq 1). Also evident by  $^1\text{H}$  NMR analysis is  $\text{HClSiL}^{\text{N}_2}$ , identified by comparison to an authentic sample.



Use of 1 equiv of silylene results in 50% conversion; with 2 equiv, quantitative reaction is effected, and **2** can be isolated as an air-sensitive yellow precipitate in >80% yield. The same products form more slowly at RT, and no intermediates are spectroscopically observable.  $^{29}\text{Si}\{^1\text{H}\}$  NMR analysis of **2** reveals a triplet at 105.7 ppm, supporting identification as a Ru-silylene species

containing two phosphine ligands. The relatively small coordination shift (cf.  $\delta$  78 for the free ligand) is in keeping with values previously reported for complexes of these stable silylenes.<sup>2-4,6</sup> The characteristic singlet at 6.75 ppm for the equivalent aromatic protons in free  $\text{SiL}^{\text{N}_2}$  is replaced in **2** by an AB quartet ( $\delta_{\text{H}}$  6.33, 6.17;  $J_{\text{HH}} = 3.8$  Hz), indicating an unsymmetrical coordination environment for the silylene ligand within **2**.  $^{31}\text{P}\{^1\text{H}\}$  NMR reveals a pair of doublets separated by ca. 80 ppm, with an unprecedentedly large coupling constant for a chelating diphosphine containing a four-carbon backbone ( $\delta$  60.2,  $-10.3$ ;  $J_{\text{PP}} = 263$  Hz). The strong P–P coupling implies an unexpected trans disposition of inequivalent phosphorus atoms, while the large peak separation indicates the presence of two different ring sizes. Phosphine ligands within four-membered chelate rings normally resonate 50–100 ppm upfield of those in five- and seven-membered chelates or monodentate phosphines.<sup>22</sup> The observed pattern finds precedent in bis(phosphine) systems in which one  $\text{PPh}_3$  ligand is orthometalated to give a four-membered  $\text{Ru-P-C-C}$  ring at  $\sim 0$  ppm, and a second, trans,  $\text{PPh}_3$  is a simple  $\eta^1$ -donor ligand at a “normal” chemical shift value of  $\sim 50$  ppm.<sup>22</sup> The presence of both four- and five-membered rings in **2** was confirmed by X-ray crystallographic analysis, which reveals an unprecedented attack of the metal on the four-carbon backbone of the dcybp ligand. We<sup>15</sup> and others<sup>23-25</sup> have reported the high activity of ruthenium cyclohexylphosphine systems toward attack on saturated C–H bonds under mild conditions. While intramolecular bond activation typically involves the cyclohexyl rings, formation of **2** clearly shows that for diphosphines forming sufficiently flexible chelate rings attack on the carbon backbone is also possible. Agostic interactions between Ru and  $\alpha$ -methylene groups of bound  $\text{Ph}_2\text{P}(\text{CH}_2)_4\text{PPh}_2$  (bis(diphenyl)phosphinobutane, dppb) have been described within a sterically congested bis(dppb) complex, resulting in deuterium incorporation into the four-carbon backbone on treatment with  $\text{D}_2$ .<sup>26</sup> Interception of the oxidative-addition product in **2** may result from facile abstraction of HCl by the basic silylene moiety.

At 185 K, the downfield  $^{31}\text{P}$  NMR signal for **2** resolves into two distinct doublets of approximately equal intensity ( $\delta$  62.2,  $J_{\text{PP}} = 274$  Hz;  $\delta$  54.3,  $J_{\text{PP}} = 260$  Hz), while the upfield doublet broadens into two poorly resolved, overlapping doublets centered at  $-10$  ppm. The corresponding solid-state spectrum shows only one of these sets of doublets ( $\delta$  56.2,  $-11.6$ ;  $J = 267$  Hz; the <2 ppm chemical shift difference between the solid-state and low-temperature data is not considered significant<sup>27</sup>). These observations are consistent with a weak agostic interaction between Ru and a  $\text{Bu}^t\text{C-H}$  bond, observable in the solid state, but favored only at low temperature in solution. An agostic  $\nu(\text{C-H})$  band is found in the solid-state IR spectrum, but not in solution; X-ray evidence for such an interaction is presented

(22) Garrou, P. E. *Chem. Rev.* **1981**, *81*, 229.

(23) Chaudret, B.; Dagnac, P.; Labroue, D.; Sabo-Etienne, S. *New J. Chem.* **1996**, *20*, 1137.

(24) Leitner, W.; Six, C. *Chem. Ber.* **1997**, *130*, 555.

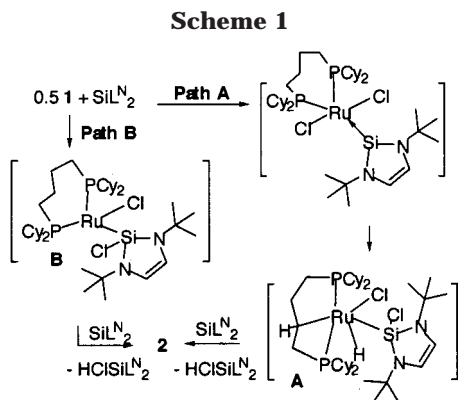
(25) Six, C.; Gabor, B.; Gorls, H.; Mynott, R.; Philipps, P.; Leitner, W. *Organometallics* **1999**, *18*, 3316.

(26) Ogasawara, M.; Saburi, M. *Organometallics* **1994**, *13*, 1911.

(27) Beml, L.; Clark, H. C.; Davies, J. A.; Fyfe, C. A.; Wasylishen, R. E. *J. Am. Chem. Soc.* **1982**, *104*, 438.

(20) Blessing, R. *Acta Crystallogr.* **1995**, *A51*, 33.

(21) Sheldrick, G. M. *Bruker AXS*; Madison, WI, 1997.



below. An alternative silyl–silylene equilibrium process<sup>5</sup> involving reversible migration of chloride ligand to Si may be discounted on the basis of the near-identity of the <sup>31</sup>P NMR values for the two species.

**Mechanism.** The observed requirement for 2 equiv of SiLN<sub>2</sub> per Ru in the synthesis of **2** results from consumption of 1 equiv of the basic silylene ligand as HClSiLN<sub>2</sub>, as noted above. Coordination of SiLN<sub>2</sub> as a simple donor ligand (Scheme 1, path A) may generate sufficient steric pressure to trigger oxidative addition of a diphosphine C–H bond to the electron-rich metal center, accompanied by insertion of silylene into the Ru–Cl bond. Reductive elimination of HClSiLN<sub>2</sub> from Ru(IV) intermediate **A**, with coordination of a second silylene, would afford **2**. The Ru(IV) oxidation state is readily accessible in species containing strongly basic donor ligands. Examples include Cp\*<sub>2</sub>Ru silyl hydrides<sup>3,9,10,28</sup> as well as alkylphosphine complexes.<sup>29,30</sup> Precedent also exists, however, for direct insertion of SiLN<sub>2</sub> into a M–Cl bond (path B).<sup>5</sup> In view of the bulk of the phosphine and silyl ligands, intermediate **B** may be more likely than six-coordinate **A**. Crystallographic evidence for four-coordinate Ru within a sterically encumbered ligand environment was recently reported.<sup>31</sup>

X-ray quality crystals of **2** were obtained by slow evaporation of a benzene solution. The complex (Figure 1) exists as two crystallographically equivalent mirror images. The short nonbonding distance between the Ru center and a methyl carbon of one of the Bu<sup>t</sup> groups (2.899(7) Å) suggests an agostic interaction between the C–H bond and the Ru center. The solid-state geometry about the Ru center is thus best described as distorted octahedral, with the dcybp ligand functioning as an η<sup>3</sup>-donor, oriented in a *mer* fashion with the activated carbon of the C<sub>4</sub> backbone trans to the agostic interaction. The SiLN<sub>2</sub> ligand is trans to the remaining chloride ligand (Si–Ru–Cl ∼ 160°) and is planar at silicon (sum of bond angles = 359.81°, ∼ 360°). The Ru–Si bond distance of 2.2264(11) Å is to our knowledge the shortest known, being slightly less than the value of 2.238(2) Å

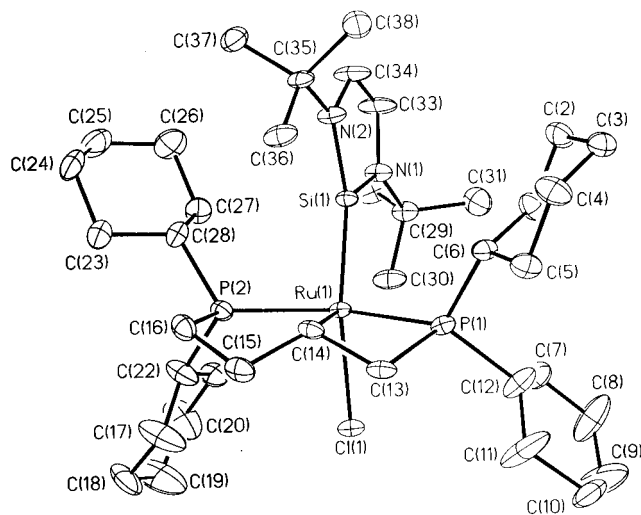


**Figure 1.** ORTEP diagram of RuCl(η<sup>3</sup>-dcpyp)(SiLN<sub>2</sub>), **2**, with thermal ellipsoids shown at the 30% probability level. Hydrogen atoms, solvate molecules, and mirror image complex omitted for clarity. An ORTEP diagram of the mirror image complex is included in the Supporting Information.

reported for [Cp\*(Me<sub>3</sub>P)<sub>2</sub>Ru=SiMe<sub>2</sub>][B(C<sub>6</sub>F<sub>5</sub>)<sub>4</sub>].<sup>10</sup> π-Bonding between the metal and silicon centers is improbable, however, as discussed in more detail below.

Of note in the structure are the Ru–Si–N angles, which differ by nearly 40°. This difference reflects a 20° “tipping” of the SiLN<sub>2</sub> ligand from an axis drawn from Ru through Si and the centroid of the silylene ring. Like the 20° deviation from linearity in the Cl–Ru–Si angle, this distortion minimizes steric interactions between the Bu<sup>t</sup> group on N(2) and the cyclohexyl substituents, while promoting development of the Ru/C–H agostic interaction.

**Frontier Orbital Analysis.** The emerging picture of the SiLN<sub>2</sub> moiety is of a predominantly σ-donor ligand, in which internal stabilization of the silylene is effected by donation of electron density from the lone pairs on nitrogen into the empty Si p orbital.<sup>32,33</sup> Consistent with minimal electronic perturbation of the ligand within **2**, relative to free SiLN<sub>2</sub>, is the small <sup>29</sup>Si NMR coordination shift. The observed value of δ 106 is well within the δ 97.5–146.9 range described for complexes containing primarily σ-donor silylenes.<sup>2–6,10</sup> Furthermore, despite the very short Ru–Si bond distance, the bond lengths within the SiLN<sub>2</sub> fragment itself are very slightly shorter than those of the free silylene.<sup>12</sup> Examination of the frontier molecular orbitals supports this analysis. For complex **2**, assuming an octahedral solid-state geometry, a d<sub>xy</sub>, d<sub>xz</sub>, or d<sub>yz</sub> orbital must constitute the HOMO. Ruthenium–silylene back-bonding requires localization of the HOMO on d<sub>xy</sub>, and the LUMO on a vacant Si p orbital (the d<sub>xz</sub> and d<sub>yz</sub> orbitals are orthogonal to the Si p orbital, precluding overlap). Density functional theory calculations<sup>17</sup> carried out on intact **2** suggest that while the HOMO has the appropriate symmetry, the LUMO is localized not on Si but on Ru and, in part, on the Ru–C bond. The HOMO–LUMO gap is approximately 4 eV. The cumulative evidence thus supports identifica-

(28) (a) Djurovich, P. I.; Carroll, P. J.; Berry, D. H. *Organometallics* **1994**, *13*, 2551. (b) Wada, H.; Tobita, H.; Ogino, H. *Organometallics* **1997**, *16*, 3870. (c) Wada, H.; Tobita, H.; Ogino, H. *Organometallics* **1997**, *16*, 2200. (d) Mitchell, G. P.; Tilley, T. D. *J. Am. Chem. Soc.* **1997**, *119*, 11236.

(29) Rodriguez, V.; Sabo-Etienne, S.; Chaudret, B.; Thorburn, J.; Ulrich, S.; Limbach, H.-H.; Eckert, J.; Barthelat, J.-C.; Hussein, K.; Marsden, C. J. *Inorg. Chem.* **1998**, *37*, 3475.

(30) Drouin, S. D.; Yap, G. P. A.; Fogg, D. E. *Inorg. Chem.* **2000**, *39*, 5412.

(31) Sanford, M. S.; Henling, L. W.; Day, M. W.; Grubbs, R. H. *Angew. Chem., Int. Ed.* **2000**, *39*, 3451.

(32) Denk, M.; Green, J. C.; Metzler, N.; Wagner, M. J. *J. Chem. Soc., Dalton Trans.* **1994**, 2405.

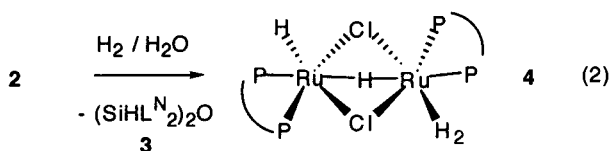
(33) West, R.; Denk, M. *Pure Appl. Chem.* **1996**, *68*, 785.

tion of the silylene ligand as a  $\sigma$ -donor to Ru, the very short Ru–Si distance likely resulting from the strong electrostatic interaction between this electrophilic ligand and the electron-rich metal center.

### Reaction of Silylene Complex with Hydrogen.

The low reactivity reported for  $\text{Cp}^*\text{Ru}(\text{SiX}_2)(\text{PMe}_3)_2]^+$  ( $\text{X} = \text{SMe}_2, \text{Me}$ ) toward nonpolar, unsaturated substrates<sup>11</sup> and  $\text{H}_2$ <sup>10</sup> is unsurprising given the coordinative saturation of the metal in these complexes. Such reactions are of keen interest in view of (1) the possible role of silylene intermediates in organosilicon transformations involving evolution or reaction with  $\text{H}_2$ ,<sup>7</sup> and (2) the more recent interest in silylene ligands as phosphine equivalents.<sup>2,4</sup> The accessibility of coordinatively unsaturated **2** affords a means of probing the reactivity of the silylene ligand toward displacement and/or hydrogenolysis. Investigations of the reactivity of **2** toward  $\text{H}_2$  and CO were thus undertaken.

Reaction of **2** under 1 atm  $\text{H}_2$  is very slow at room temperature, with <50% conversion after 1 week, but can be driven to completion within 24 h at 50 °C. No intermediates are evident by <sup>31</sup>P NMR analysis. The Ru product is spectroscopically identical (<sup>1</sup>H and <sup>31</sup>P NMR) to hydridochloro species **4**, prepared in independent work by treating **1** with potassium tri(*sec*-butyl)borohydride.<sup>19</sup> Loss of the silicon ligand is further supported by X-ray crystallographic analysis of a decomposition product serendipitously obtained on attempted isolation of **4** from the reaction mixture (vide infra). <sup>1</sup>H, <sup>13</sup>C, and <sup>29</sup>Si NMR analysis of the sole Si-containing product permits its identification as  $[\text{L}^{\text{N}}_2\text{Si}(\text{H})]_2\text{O}$  **3**,<sup>18</sup> suggesting that reaction involves both hydrogenolysis and, more unexpectedly, hydrolysis. (The latter may occur, despite the use of standard “anhydrous” Schlenk techniques, from use of a Deoxo cartridge to scavenge trace oxygen from the  $\text{H}_2$  stream by catalytic conversion to water; no evidence of hydrolysis was observed under  $\text{N}_2$  atmosphere.) Implication of water in this transformation is confirmed by complete conversion of **2** to **4** and siloxane **3**, without heating, on addition of stoichiometric quantities of  $\text{H}_2\text{O}$  under  $\text{H}_2$ . Other side-products form on use of water alone; these are partially converted to **4** and siloxane on subsequent exposure to  $\text{H}_2$ . Reaction with both water and  $\text{H}_2$  is thus required to generate the observed hydride and siloxane products. The overall reaction of **2** is indicated in eq 2.



The silylene–siloxane transformation is indicated by replacement of the olefinic doublets for **2** by two new signals in the olefinic/silyl region. A singlet at 5.95 ppm is assigned to a silyl proton on the basis of its correlation with the <sup>29</sup>Si peak (<sup>1</sup>H–<sup>29</sup>Si HMQC; <sup>1</sup>J<sub>SiH</sub> = 278 Hz), supported by the absence of an H–C correlation in the corresponding <sup>1</sup>H–<sup>13</sup>C HMQC experiment. Also evident in this region (5.80 ppm) is one olefinic signal, which at 500 MHz is resolved into a doublet with long-range coupling to silicon (<sup>J</sup><sub>SiH</sub> = 2 Hz; <sup>1</sup>H/<sup>29</sup>Si HMBC). This resonance correlates with a <sup>13</sup>C methine signal at  $\delta$  111.8, itself assigned by <sup>13</sup>C DEPT. <sup>29</sup>Si INEPT analysis

### Scheme 2

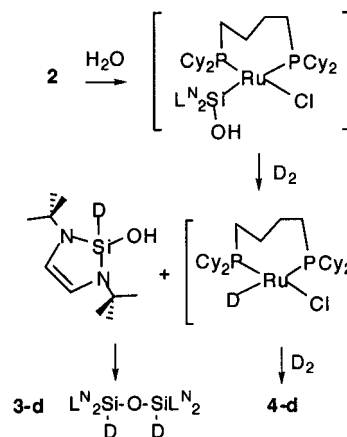


### Table 1. Crystal Data and Structure Refinement for **2**

empirical formula	C <sub>44</sub> H <sub>77</sub> ClN <sub>2</sub> P <sub>2</sub> RuSi
fw	860.63
temperature	203(2) K
wavelength	0.71073 Å
cryst syst, space group	monoclinic, <i>Pc</i>
unit cell dimens	<i>a</i> = 13.503(1) Å, $\alpha$ = 90° <i>b</i> = 17.697(2) Å, $\beta$ = 105.742(2)° <i>c</i> = 20.110(2) Å, $\gamma$ = 90°
volume	4625.3(8) Å <sup>3</sup>
<i>Z</i> , calcd density	4, 1.236 mg/m <sup>3</sup>
abs coeff	0.522 mm <sup>-1</sup>
<i>F</i> (000)	1840
cryst size	0.2 × 0.2 × 0.1 mm
$\theta$ range for data collection	1.15–28.83°
limiting indices	–17 ≤ <i>h</i> ≤ 18, 0 ≤ <i>k</i> ≤ 23, –26 ≤ <i>l</i> ≤ 25
no. of reflns collected/unique	36492/17571 [ <i>R</i> (int) = 0.0496]
completeness to $\theta$ = 28.83°	92.3%
abs corr	semiempirical from equivalents
max. and min. transmn	0.928076 and 0.613589
refinement method	full-matrix least-squares on <i>F</i> <sup>2</sup>
no. of data/restraints/params	17571/2/895
goodness-of-fit on <i>F</i> <sup>2</sup>	1.021
<i>R</i> <sup>a</sup>	0.0388
<i>R</i> <sub>w</sub> <sup>b</sup>	0.0513

$$^a R = \sum ||F_o| - |F_c|| / \sum |F_o|. \quad ^b R_w = [\sum w\delta^2 / \sum wF_o^2]^{1/2}.$$

of the product mixture reveals one <sup>29</sup>Si resonance ( $\delta$  –57.6), confirming identification of this species as siloxane dimer  $[\text{L}^{\text{N}}_2\text{Si}(\text{H})]_2\text{O}$  **3**.<sup>18</sup>

Jutzi and co-workers recently described the synthesis of metallocsilanol species  $\text{Cp}_2\text{Mo}(\text{H})(\text{SiL}^{\text{N}}_2\text{OH})$ , via controlled hydrolysis of  $\text{Cp}_2\text{Mo}(\text{SiL}^{\text{N}}_2)$ .<sup>6</sup> An analogous silyl hydride complex,  $\text{Cp}_2\text{Mo}(\text{H})(\text{SiHL}^{\text{N}}_2)$ , was obtained by insertion of  $\text{SiL}^{\text{N}}_2$  into an M–H bond of  $\text{Cp}_2\text{MH}_2$  ( $\text{M} = \text{Mo}, \text{W}$ ).<sup>6</sup> Interestingly, **2** appears to be stable toward hydrogenolysis alone, despite the presence of the Ru–C and silylene entities and the coordinative unsaturation of the metal. Thus, we see no products that can be attributed to reaction with  $\text{H}_2$  alone: while this might in principle be accounted for by a (**2** +  $\text{H}_2$ ) equilibrium that lies far to the left, reaction with  $\text{D}_2$  would then be expected to effect incorporation of D into the dcypb backbone (via reductive elimination of the activated C–H bond). However, labeling studies carried out with  $\text{D}_2$  show no <sup>2</sup>H aliphatic signals prior to emergence of <sup>31</sup>P NMR signals for **4-d**. In conjunction with the stoichiometric reactions with  $\text{H}_2\text{O}/\text{H}_2$  described above, this implies that reaction of **2** with water precedes reaction with  $\text{D}_2$  (or  $\text{H}_2$ ). <sup>2</sup>H NMR analysis indicates that



**Table 2. Selected Bond Lengths (Å) and Angles (deg) for 2<sup>a</sup>**

Ru(1)–Si(1)	2.2264(11), 2.2293(12)	Si(1)–N(1)	1.732(3), 1.725(3)
Ru(1)–C(14)	2.110(4), 2.114(4)	Si(1)–N(2)	1.734(3), 1.741(3)
Ru(1)–P(2)	2.3373(12), 2.3279(12)	N(1)–C(33)	1.388(5), 1.377(6)
Ru(1)–P(1)	2.3389(12), 2.3422(11)	N(2)–C(34)	1.399(6), 1.411(6)
Ru(1)–Cl(1)	2.4713(11), 2.4738(10)	C(33)–C(34)	1.336(6), 1.329(6)
N(1)–Si(1)–N(2)	90.60(17), 90.61(17)	C(14)–Ru(1)–Si(1)	104.45(12), 103.76(12)
N(1)–Si(1)–Ru(1)	116.06(12), 116.42(12)	C(14)–Ru(1)–P(1)	69.21(13), 69.50(12)
N(2)–Si(1)–Ru(1)	153.15(13), 152.97(13)	C(14)–Ru(1)–P(2)	83.05(13), 83.68(12)
P(2)–Ru(1)–P(1)	152.11(4), 152.91(4)	C(14)–Ru(1)–Cl(1)	95.16(12), 95.87(12)

<sup>a</sup> The second value is the corresponding value for the mirror image complex.

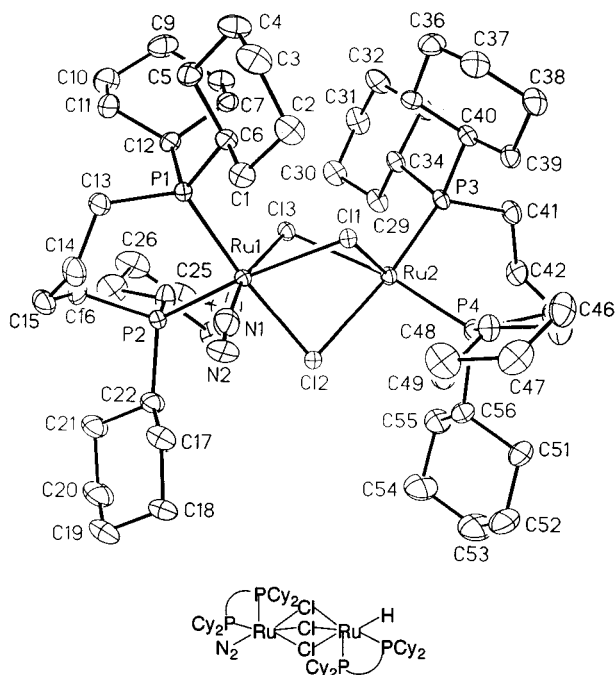


**Figure 2.** ORTEP diagram of [(dcp)Ru( $\mu$ -Cl)<sub>3</sub>Ru(dcp)(N<sub>2</sub>)]**5**, with thermal ellipsoids shown at the 30% probability level. Hydrogen atoms and solvate molecule omitted for clarity. Line diagram shows position of hydride (not located crystallographically).

the siloxane product formed in these reactions, whether at RT or by thermolysis, is solely [L<sup>N</sup><sub>2</sub>Si(D)]<sub>2</sub>O. Consistent with these observations is the mechanism of Scheme 2, in which evolution of siloxane results from successive reaction of **2** with H<sub>2</sub>O and D<sub>2</sub> (H<sub>2</sub>). Nucleophilic attack of water on bound silylene may afford a  $\eta^1$ -silanol hydride intermediate,<sup>6</sup> which reductively eliminates to yield a silanol species containing a simple  $\eta^2$ -diphosphine ligand. Reaction with H<sub>2</sub> would then liberate L<sup>N</sup><sub>2</sub>-SiD(OH) (which can then condense to form the siloxane **3**<sup>18</sup>) and a hydride species. Dimerization of the latter and reaction with D<sub>2</sub> would give **4**. Not indicated in Scheme 2 are miscellaneous reactions involving scrambling of the deuterium label into the Cy rings and/or dcpb backbone. Exchange of Ru–D into phosphine cyclohexyl C–H bonds is common,<sup>15,23–25</sup> while exchange with C<sub>4</sub>-methylene backbones in a dppb complex<sup>26</sup> was noted above.

**Crystal Structure of 5.** We recently described the susceptibility of the parent dcpb complex **1** to intramolecular dehydrogenation on removal of H<sub>2</sub> atmosphere or concentration to dryness.<sup>15</sup> Dehydrogenation likewise results from attempted isolation of **4**, as indicated by the emergence of olefinic signals and a singlet for dissolved H<sub>2</sub>. Such processes may thus be a general

**Table 3. Crystal Data and Structure Refinement for 5**

empirical formula	C <sub>62</sub> H <sub>109</sub> Cl <sub>3</sub> N <sub>2</sub> P <sub>4</sub> Ru <sub>2</sub>
fw	1314.88
temperature	203(2) K
wavelength	0.71073 Å
cryst syst, space group	triclinic, $P\bar{1}$
unit cell dimens	$a = 11.6220(9)$ Å, $\alpha = 89.7230(10)^\circ$ $b = 13.5699(10)$ Å, $\beta = 86.8370(10)^\circ$ $c = 22.7781(17)$ Å, $\gamma = 66.5080(10)^\circ$
volumel	3289.0(4) Å <sup>3</sup>
Z, calcd density	2, 1.328 mg/m <sup>3</sup>
abs coeff	0.716 mm <sup>-1</sup>
F(000)	1388
cryst size	0.20 × 0.10 × 0.05 mm
$\theta$ range for data collection	1.64–28.71°
limiting indices	–15 ≤ $h$ ≤ 15, –17 ≤ $k$ ≤ 17, 0 ≤ $l$ ≤ 30
no. of reflns collected/ unique	25795/14910 [ $R(\text{int}) = 0.0404$ ]
completeness to $\theta = 28.71$	87.6%
abs corr	semiempirical from equivalents
max. and min. transmn	0.928076 and 0.828149
refinement method	full-matrix least-squares on $F^2$
no. of data/restraints/ params	14 910/0/658
goodness-of-fit on $F^2$	1.028
$R^a$	0.0487
$R_w^b$	0.0971

$$^a R = \sum ||F_o| - |F_c|| / \sum ||F_o|. \quad ^b R_w = [\sum w\delta^2 / \sum wF_o^2]^{1/2}.$$

**Table 4. Selected Bond Lengths (Å) and Angles (deg) for 5**

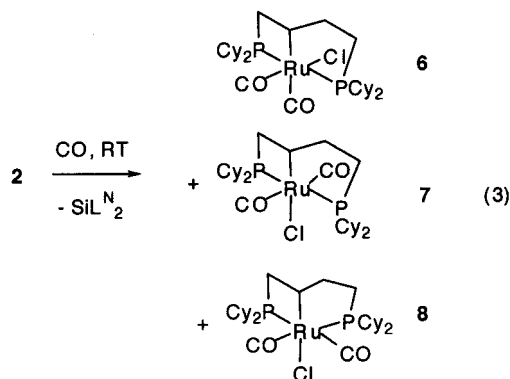
N(1)–N(2)	1.110(5)	Ru(1)–Cl(1)	2.4840(10)
Ru(1)–N(1)	1.898(6)	Ru(1)–Cl(2)	2.4793(10)
Ru(1)–P(1)	2.3225(11)	Ru(1)–Cl(3)	2.4636(10)
Ru(1)–P(2)	2.3369(11)	Ru(2)–Cl(1)	2.6092(10)
Ru(2)–P(3)	2.2352(11)	Ru(2)–Cl(2)	2.5403(10)
Ru(2)–P(4)	2.2419(12)	Ru(2)–Cl(3)	2.5107(11)
N(2)–N(1)–Ru(1)	173.0(4)	P(3)–Ru(2)–P(4)	96.67(4)
N(1)–Ru(1)–P(1)	92.46(13)	Ru(1)–Cl(1)–Ru(2)	83.41(3)
N(1)–Ru(1)–P(2)	94.82(12)	Ru(1)–Cl(2)–Ru(2)	84.95(3)
P(1)–Ru(1)–P(2)	93.46(4)	Ru(1)–Cl(3)–Ru(2)	85.91(3)

characteristic of Ru-dcpb complexes in coordinatively unsaturated environments. That other, intermolecular, processes are involved, at least in decomposition of **4**, is suggested by the presence of an additional chloride ligand in [(dcp)Ru( $\mu$ -Cl)<sub>3</sub>Ru(dcp)(N<sub>2</sub>)]**5**. The latter species, identified by X-ray crystallography, crystallized on attempted isolation of **4** following reaction of **2** with H<sub>2</sub>/H<sub>2</sub>O. A benzene solution containing the products was stripped to dryness, and the residue was washed with a few drops of hexanes, then redissolved in benzene. Crystals of **5** deposited on slow evaporation under N<sub>2</sub>. Many other species are also present in solution, as judged by <sup>31</sup>P and <sup>1</sup>H NMR. An ORTEP representation of **5** (accompanied by a line drawing) appears in Figure 2, with crystallographic and selected structural parameters in Tables 3 and 4, respectively.

Complex **5** adopts a triply chloride-bridged diruthenium structure, in which the coordination geometry at each metal center is distorted octahedral, taking into consideration the presence of a hydride ligand on Ru(2). The structure is unsymmetrical, with Ru(1) bearing an end-bound dinitrogen ligand. Location of the hydride ligand on Ru(2) is inferred from the very long Ru(2)–Cl(1) bond distance (2.6092(10) Å, vs the average Ru–Cl bond length of 2.496(10) Å). The presence of this sterically undemanding ligand permits a larger bite angle of the diphosphine ligand subtended at Ru(2), vs the more sterically crowded Ru(1) (96.7°, vs 93.5°). <sup>1</sup>H NMR analysis of the isolated solid shows several hydridic resonances. While a search of the Cambridge Crystallographic Database reveals no direct analogues of the “Ru( $\mu$ -Cl)<sub>3</sub>Ru(H)” framework, the structural parameters for **5** are very similar to data reported for the closely related complex  $[(\eta^2\text{-H}_2)(\text{dppb})\text{Ru}(\mu\text{-Cl})_3\text{RuCl}(\text{dppb})]$ ,<sup>34</sup> Ruthenium–phosphorus, –nitrogen, and –chloride distances (other than for the chloride trans to hydride) tally closely with the values reported, as do angles within the Ru–P–Cl skeleton.

**Reaction with Carbon Monoxide.** Suspensions of **2** react with CO within hours to give a clear pale yellow solution containing free SiL<sub>N</sub><sub>2</sub> and three isomeric ruthenium carbonyl derivatives, **6–8**. The high solubility of the Ru products hampered their separation from each other and from free silylene. Displacement of SiL<sub>N</sub><sub>2</sub> is indicated by the complete disappearance of the <sup>1</sup>H NMR AB quartet for the bound ligand and emergence of a prominent singlet for free silylene (6.75 ppm). Retention of the  $\eta^3$ -dcypb framework in **6–8** is indicated by the characteristically large <sup>31</sup>P{<sup>1</sup>H} NMR peak separations ( $\Delta\delta_{\text{P}} \sim 100$  ppm). Unambiguous identification of all three as isomeric bis(CO) derivatives (eq 3) is provided by <sup>31</sup>P NMR analysis of their <sup>13</sup>CO isotopomers. <sup>31</sup>P–<sup>13</sup>C splitting results in transformation of each doublet present in the original <sup>31</sup>P NMR spectrum into a doublet of doublets (**6**, **7**) or a doublet of triplets (**8**). Isomers **6** and **7** contain trans-disposed phosphorus ligands, as indicated by their large <sup>2</sup>J<sub>PP</sub> values (~250 Hz). Distortion from the idealized structures represented in eq 3 is indicated by the observation of four inequivalent <sup>13</sup>CO resonances for **6** + **7** (as well as two for **8**). Consequently, **6** and **7** cannot be distinguished by spectroscopic data.

A structural distinction between these products and isomer **8** is indicated by the much smaller <sup>2</sup>J<sub>PP</sub> value for the latter (164 Hz), which implies a smaller P–Ru–P dihedral angle. That the angle is still much larger than 90° is indicated, however, by comparison of this coupling constant to “normal” cis <sup>2</sup>J<sub>PP</sub> values of 11–50 Hz.<sup>22</sup> A highly distorted octahedral arrangement, with the diphosphine ligand taking up a geometry intermediate



between the meridional extreme of **6/7** and a true facial arrangement, is thus suggested.

### Conclusions

The foregoing describes an unusual example of a silylene moiety found within a coordinatively unsaturated ligand environment containing chloride and phosphine ligands, in which a novel  $\eta^3$ -coordination mode for the chelating diphosphine results from activation of an sp<sup>3</sup> C–H bond within the tetramethylene backbone. Solid-state and low-temperature NMR data, supported by crystallographic analysis, suggest a coordinatively saturated structure, in which an agostic interaction occupies the sixth coordination site. Confirmation of the accessibility of this site in solution, and indications of the noninnocent behavior of the silylene ligand, comes from the observed reactivity toward both H<sub>2</sub>/H<sub>2</sub>O and CO. Displacement of silylene by CO is facile at room temperature, giving access to novel  $\eta^3$ -dcypb carbonyl complexes. Hydrolysis and hydrogenolysis afford a simple  $\eta^2$ -dcypb complex, with elimination of bound silylene as siloxane. These results join several recent examples in suggesting that—in contrast to current views of the analogous, Arduengo-type carbenes—the SiL<sub>N</sub><sub>2</sub> ligand can readily participate in reactions at transition-metal metal centers.

**Acknowledgment.** Helpful discussions with Professor Michael Denk (Toronto) are acknowledged with thanks. This work was supported by the Natural Sciences and Engineering Research Council of Canada, the Canada Foundation for Innovation, and the Ontario Innovation Trust.

**Supporting Information Available:** Tables of crystal data collection and refinement parameters, atomic coordinates, bond lengths and angles, anisotropic displacement parameters, and hydrogen coordinates for **2** (and its mirror image complex) and **5**. An ORTEP diagram for the mirror image of **2** is also included. This material is available free of charge via the Internet at <http://pubs.acs.org>.

(34) MacFarlane, K. S.; Thorburn, I. S.; Cyr, P. W.; Chau, D. E. K. Y.; Rettig, S. J.; James, B. R. *Inorg. Chim. Acta* **1998**, *270*, 130–144.